

Published in final edited form as:

*Chem Res Toxicol.* 2013 April 15; 26(4): 564–574. doi:10.1021/tx400001x.

## Protein Targets of Thioacetamide Metabolites in Rat Hepatocytes

Yakov M. Koen<sup>1</sup>, Diganta Sarma<sup>1</sup>, Heather Hajovsky<sup>1</sup>, Nadezhda A. Galeva<sup>2</sup>, Todd D. Williams<sup>2</sup>, Jeffrey L. Staudinger<sup>3</sup>, and Robert P. Hanzlik<sup>1,\*</sup>

<sup>1</sup>Department of Medicinal Chemistry, The University of Kansas, Lawrence, Kansas 66045

<sup>2</sup>Mass Spectrometry Laboratory, The University of Kansas, Lawrence, Kansas 66045

<sup>3</sup>Department of Pharmacology & Toxicology, The University of Kansas, Lawrence, Kansas 66045

### Abstract

Thioacetamide (TA) has long been known as a hepatotoxicant whose bioactivation requires *S*-oxidation to thioacetamide *S*-oxide (TASO) and then to the very reactive *S,S*-dioxide (TASO<sub>2</sub>). The latter can tautomerize to form acylating species capable of covalently modifying cellular nucleophiles including phosphatidylethanolamine (PE) lipids and protein lysine side chains. Isolated hepatocytes efficiently oxidize TA to TASO but experience little covalent binding or cytotoxicity because TA is a very potent inhibitor of the oxidation of TASO to TASO<sub>2</sub>. On the other hand hepatocytes treated with TASO show extensive covalent binding to both lipids and proteins accompanied by extensive cytotoxicity. In this work, we treated rat hepatocytes with [<sup>14</sup>C]-TASO and submitted the mitochondrial, microsomal and cytosolic fractions to 2DGE which revealed a total of 321 radioactive protein spots. To facilitate the identification of target proteins and adducted peptides we also treated cells with a mixture of TASO/[<sup>13</sup>C<sub>2</sub>D<sub>3</sub>]-TASO. Using a combination of 1DGE- and 2DGE-based proteomic approaches, we identified 187 modified peptides (174 acetylated, 50 acetimidoylated and 37 in both forms) from a total of 88 non-redundant target proteins. Among the latter, 57 are also known targets of at least one other hepatotoxin. The formation of both amide- and amidine-type adducts to protein lysine side chains is in contrast to the exclusive formation of amidine-type adducts with PE phospholipids. Thiobenzamide (TB) undergoes the same two-step oxidative bioactivation as TA, and it also gives rise to both amide and amidine adducts on protein lysine side chains but only amidine adducts to PE lipids. Despite their similarity in functional group chemical reactivity, only 38 of 62 known TB target proteins are found among the 88 known targets of TASO. The potential roles of protein modification by TASO in triggering cytotoxicity are discussed in terms of enzyme inhibition, protein folding and chaperone function, and the emerging role of protein acetylation in intracellular signaling and the regulation of biochemical pathways.

### Introduction

Thioacetamide (TA) and thiobenzamide (TB) are representatives of a large group of thiocarbonyl compounds, many of which are hepatotoxic.<sup>1–6</sup> In rats, the toxicity of TB stems from the covalent modification of lysine side chains on cellular proteins by its reactive *S,S*-dioxide metabolite,<sup>7</sup> accompanied by extensive modification of the amine group on cellular

\*Address correspondence to: Dr. Robert P. Hanzlik, University of Kansas, Department of Medicinal Chemistry, Room 4048 Malott Hall, 1251 Wescoe Hall Drive, Lawrence, KS 66045, Tel. 785-864-3750, rhanzlik@ku.edu.

Supporting Information

Tables S1–S3 and Figures S1–S6 (13 pages, 7.8 MB); Table S4 and Figure S7 (32 MB). This material is available free of charge via the Internet at <http://pubs.acs.org>.

PE phospholipids.<sup>8</sup> Among protein lysine groups both benzamide and benzamidine modifications are formed, whereas only benzamidine modifications are observed on the PE phospholipids.

TA and its initial metabolite thioacetamide S-oxide (TASO) elicit a variety of hepatotoxic responses in rats depending on the dose and duration of administration.<sup>5, 9</sup> TASO is strongly cytotoxic to isolated rat hepatocytes in vitro, yet TA is not, despite the fact that rat hepatocytes readily convert TA to TASO. This is due to the fact that TA is a potent inhibitor of the oxidation of TASO to its reactive S,S-dioxide metabolite TASO<sub>2</sub>.<sup>5</sup> By analogy with TB, the metabolism of TA and TASO in vivo leads to the formation of acetamide derivatives on protein lysine side chains.<sup>10, 11</sup> In isolated hepatocytes, metabolism of TASO leads to extensive modification of both protein lysine side chains and the amine groups of PE lipids.<sup>6</sup> The lysine adducts comprise both acetamide and acetamidine modifications, whereas the PE lipid adducts comprise exclusively acetamidine groups. In hepatocytes, this covalent binding precedes the appearance of cytotoxic effects, and both are prevented by TA and other compounds that block the oxidative metabolism of TASO.<sup>5</sup>

The main objectives of this work were to characterize the reactive metabolite target proteome of TASO in rat hepatocytes, to compare it to those of other known hepatotoxicants, and to identify individual sites of protein modification and the structures of the adducts formed. We incubated freshly isolated rat hepatocytes with either [<sup>14</sup>C]-TASO or [<sup>13</sup>C<sub>2</sub>D<sub>3</sub>]-TASO and analyzed subcellular fractions by 1D- and 2D gel electrophoresis followed by tryptic digestion and LC-MS/MS analysis. Herein we report the identification of 88 proteins targeted by the reactive metabolite of TASO. This is the largest set of target proteins known for any single bioactivated chemical.<sup>12</sup> While many reactive metabolite targets have been identified at the protein level,<sup>12</sup> the characterization and sequencing of adducts at the peptide level has only rarely been achieved. However, because of the efficiency of cellular protein modification by TASO metabolites, we are also able to report the identification and sequencing of peptides comprising 187 different sites of adduction among the 88 TASO metabolite target proteins. Finally, we compare the list of TASO metabolite targets to the range of others in the reactive metabolite target protein database<sup>12</sup> and comment on the potential contribution of their modification to the ensuing toxicity.

## Experimental Procedures

### Materials

TASO, [<sup>14</sup>C]-TASO (1.95 Ci/mol) and [<sup>13</sup>C<sub>2</sub>D<sub>3</sub>]-TASO were synthesized according to a literature procedure.<sup>13</sup> Deionized water (resistivity 18.2 MH/cm) was used for the preparation of all solutions and buffers. Other materials and suppliers were as follows: Collagenase type IV, Percoll and 4-vinylpyridine (sigmaaldrich.com); HPLC grade solvents and analytical grade inorganic salts (fishersci.com); Dulbecco's modified Eagle's medium (DMEM) and phosphate-buffered saline (PBS, pH 7.4) (cellgro.com); sequencing grade trypsin (rocheusa.com); Protease Inhibitor Cocktail (PIC), Sequenal grade urea and 3-[(3-cholamidopropyl)dimethylammonio]-1-propanesulfonate (CHAPS, piercenet.com); silica gel TLC plates, type LK5DF with a pre-adsorbent loading zone (whatman.com); Tris, SDS, glycine, Sequi-blot PVDF membranes (0.2 micron pore size), Bradford reagent, and Precision Protein Standards (biorad.com); other electrophoresis supplies (gehealthcare.com).

### Preparation of Isolated Hepatocytes

Male Sprague-Dawley rats from Charles River Laboratories (criver.com) were housed in a temperature and humidity controlled room with a 12 h light/dark cycle and ad libitum access to food and water. All animal husbandry protocols were in accordance with the NIH

Guide.<sup>14</sup> Experimental procedures were approved by the University of Kansas Institutional Animal Care and Use Committee. Hepatocytes from non-induced male Sprague-Dawley rats (175–275 g) were isolated using a previously described protocol.<sup>15</sup> Initial cell viability (85–95%) was assessed using trypan blue exclusion. After isolation, the cells were transferred to the incubation medium A (DMEM supplemented with 1% (v/v) Pen-Strep, insulin (4 mg/L), 5% FBS, 100 nM dexamethasone, and 2 mM L-glutamine (all from Gibco-Invitrogen, [www.invitrogen.com](http://www.invitrogen.com))).

### Detection of acetylated proteins by western blotting

Freshly isolated hepatocytes were plated on 6-well collagen coated plates and allowed to attach for 3 hours as described,<sup>5</sup> after which the cells were treated with TASO (3 mM) in nutrient-rich WME [Williams' Medium E supplemented with 1% ITS, 1% Pen-Strep, 2 mM L-glutamine, and 100 nM dexamethasone (3.0 mL/well)] for 10, 30 or 60 min. Control (UT) cells were incubated for 60 min in the same medium without TASO. Cells were treated with RIPA lysis buffer (150 mM NaCl, 1% NP-40, 0.5% sodium deoxycholate, 0.1% SDS, 50 mM Tris, pH 8.0) supplemented with 1X protease and phosphatase inhibitors (Thermo Scientific). Cell lysates were subjected to sonication followed by centrifugation for 10 min at  $20,000 \times g$  at 4°C. Aliquots of the resulting supernatants containing identical amounts of protein were subjected to electrophoresis and transblotting as described.<sup>5</sup> Blots were then probed with a mouse monoclonal antibodies cocktail containing anti-acetylated lysine (15910) (Novus Biologicals, Cat. # NB100-78428), Ac-lysine (AKL5C1) (Santa Cruz, Cat. # sc-32268), acetylated-lysine (Ac-k-103) (Cell Signaling, Cat. # 96815), and acetylated lysine (Thermo Scientific, Cat. # MA1-2021) antibodies at a 1:2000 dilution for 2 h. The blots were then treated with HRP-conjugated anti-mouse secondary antibody (Santa Cruz, Cat#sc-2005) and Pierce ECL Western Blotting Substrate according to the manufacturer's protocol. The reaction was visualized by exposing the blots to X-ray films.

### Hepatocyte Incubations

For studies aimed at detection of adducted proteins, [<sup>14</sup>C]-TASO (10 mM, 1.95 Ci/mol) was incubated with hepatocytes freshly isolated from two rats ( $1 \times 10^7$  live cells/mL in a total volume of 1.7 or 2.3 mL, respectively, of medium A) in 50 mL round-bottom screw-cap culture tubes. Before adding the hepatocytes to the tubes, the required amounts of TASO were deposited by evaporation from a methanol solution. Incubations were shaken at 140 Hz in a water-bath at 37 °C under an atmosphere of O<sub>2</sub>/CO<sub>2</sub> (95:5) for 4–5 h. Immediately after the incubation, the medium was removed by centrifugation (3 min at 100 g) and the cell pellets were frozen at –80°C. Hepatocytes from two separate incubations were pooled to give a total of  $1 \times 10^8$  cells prior to subcellular fractionation (see below). In parallel, small scale incubations were conducted for quantitative assessment of covalent binding by protein precipitation and washing on 3MM filter paper.<sup>5</sup> For identification of protein adducts, a 10:6 mixture of [<sup>13</sup>C<sub>2</sub>D<sub>3</sub>]-TASO/TASO was substituted for radiolabeled TASO and incubations were conducted identically. Hepatocytes from four different preparations were incubated separately, centrifuged, frozen and pooled (a total of ca.  $2.5 \times 10^8$  cells) prior to their fractionation as described below.

### Preparation of Subcellular Fractions of Hepatocytes

The incubated cells were homogenized and fractionated by differential centrifugation with all procedures performed at 0–4 °C. The cell pellets were thawed and resuspended by gently pipetting with a small volume of homogenization buffer (50 mM Tris-HCl, pH 7.4, 150 mM KCl, 2 mM EDTA) containing proteinase inhibitor cocktail. The resulting suspensions were pooled and homogenized manually (15–20 pestle strokes) in a Potter-Elvehjem (glass-Teflon) tissue grinder maintained in an ice-bath. The final ratio of cell pellet/buffer was ca. 1:1.85 (v/v). The homogenate was centrifuged at  $800 \times g$  for 15 min. The resulting pellet

(cell debris/nuclei) was resuspended by pipetting with a small volume of a storage buffer (100 mM  $\text{KH}_2\text{PO}_4$  (pH 7.4), 1 mM EDTA, 1 mM DTT, 20% (v/v) glycerol). The 800g-supernatant was further centrifuged at  $9500 \times g$  for 20 min. The resulting pellet (P9-fraction, mitochondria) was resuspended as above, while the supernatant (S9 fraction) was further centrifuged at  $100000 \times g$  for 60 min. The resulting clear supernatant (S100, cytosol) was carefully removed, leaving some turbid supernatant (collected separately). The pellet (P100, microsomes) was resuspended by homogenization with storage buffer using a Teflon pestle directly within the centrifuge tubes. In experiments using  $^{14}\text{C}$ -TASO, clear cytosol was submitted to several successive rounds of ultrafiltration (Amicon Ultra-4 Ultracel-5k ultrafiltration centrifuge tubes) against 20 mM  $\text{KH}_2\text{PO}_4$  (pH 7.4) containing 0.25 mM EDTA, in order to remove soluble radiolabel. All the subcellular fractions were stored in aliquots at  $-80^\circ\text{C}$  until used.

### Electrophoresis, Phosphorimaging, and In-gel Digestion

These standard procedures were carried out essentially as described earlier.<sup>16–18</sup>

### Mass Spectrometry of Tryptic Digests and Protein Identification

Digested protein samples were analyzed by LC-MS/MS using a NanoAcquity chromatographic system (Waters Corp., Milford, MA) coupled to an LTQ-FT mass spectrometer (ThermoFinnigan, Bremen, Germany). Peptides were separated on a reverse-phase C18 column, 15 cm,  $300 \mu\text{m}$  I.D. (Thermo Acclaim PepMap300,  $300 \text{ \AA}$ ,  $5 \mu\text{m}$ ). The solvents were A (99.9%  $\text{H}_2\text{O}$  and 0.1% formic acid) and B (99.9% acetonitrile and 0.1% formic acid). A gradient was developed from 1 to 40% B in 50 min, increased to 95% B in 4 min, and held at 95% B for 5 min at a flow rate of  $10 \mu\text{L}/\text{min}$ . The NanoAcquity UPLC Console (Waters Corp., version 1.3) was used to control the injections and gradients. Data dependent acquisition method for the mass spectrometer (configured version LTQ-FT 2.2) was set up using Xcalibur software (Thermo Scientific, version 2.0). Full spectrum survey scans were acquired at a resolution of 50,000 with an Automatic Gain Control (AGC) target of  $5 \times 10^5$ . Five most abundant ions were fragmented in the LTQ with an AGC target of  $2 \times 10^3$  or a maximum ion time of 300 ms. The ion selection threshold was 500 counts. The LTQ-FT scan sequence was adapted from Olsen and Mann.<sup>19</sup>

Raw data files were converted into Mascot generic format using MassMatrix MS data file Conversion Tools (version 3.9). The data were then presented to Mascot search engine (Matrix Science, version 2.3) for peptide/protein identification using UniProtKB database (<http://www.uniprot.org>). In addition, the Sequest algorithm within Proteome Discoverer software (Thermo Scientific Inc., version 1.3) and the X!Tandem algorithm ([www.thegpm.org](http://www.thegpm.org)) were also used for identifying proteins and their adducts. Fragment ion mass tolerance was set to 0.20 Da and parent ion tolerance was set to 20.0 ppm. The pyridylethyl (+105) derivative of cysteine residues was specified as a static modification, and the “light” (+42) and “heavy” (+47) acetyl derivatives and the “light” (+41) and “heavy” (+46) acetimidoyl derivatives of lysine residues as well as of N-terminal amino acid residues were specified as variable modifications. Scaffold software (Proteome Software Inc., version 3.6) was used to combine and validate the results of protein identifications. For unmodified peptides, identifications were accepted if they could be established at greater than 95% probability as specified by the Peptide Prophet algorithm.<sup>20</sup> Additional criteria such as mass accuracy and the presence of light/heavy ion pairs in MS1 spectra were also considered for confirming identities of adducted peptides (see Results and Discussion section). Protein identifications were accepted if they could be established at greater than 99% probability and contained at least 2 identified peptides. Protein probabilities were assigned by the Protein Prophet algorithm.<sup>21</sup> Quantitative ratios of peptide adducts were derived from the

chromatographic areas of their monoisotopic peaks using Qual Browser of Xcalibur software (Thermo Scientific Inc., version 2.1).

## Results and Discussion

Freshly isolated rat hepatocytes were incubated with [ $^{14}\text{C}$ ]-TASO to facilitate locating adducts on 2D gel electrophoresis, and with [ $^{13}\text{C}_2\text{D}_3$ ]-TASO to generate adducts for mass spectral analysis. As reported previously,<sup>6</sup> TASO gives rise to high levels of adduction in both the protein fraction (20 nmol-equiv./million cells) and the lipid fraction (37 nmol-equiv./million cells). The rapidity and extent of protein acetylation in TASO-treated hepatocytes is illustrated in Figure 1 which shows a western blot of total cellular lysate proteins made using a cocktail mixture of four different anti-acetylsine monoclonal antibodies.

### Incubation of cells with [ $^{14}\text{C}$ ]-TASO

Two batches of freshly isolated hepatocytes (a total of ca.  $10^8$  live cells) were incubated with a cytotoxic concentration of [ $^{14}\text{C}$ ]-TASO (10 mM), then pooled and pelleted. After homogenization and differential centrifugation, the crude mitochondria, microsomes and cytosol fractions were found to contain 80, 86 and 125 nmol-equiv./mg protein, respectively. As expected, a majority of the radiolabel found in the cytosol was removable by ultrafiltration (Table 1); this probably represents unmetabolized TASO and its soluble metabolites. Hence, the actual covalent binding in these fractions is probably lower than suggested by these ratios of radioactivity to protein. The concentration of TASO we used causes some cytotoxicity, as reflected by ca. 50% leakage of lactic dehydrogenase into the medium (unpublished results; see also ref. 5). While this may impact the distribution of radioactivity among the subcellular fractions, it has no impact on the isolation and identification of target proteins.

Individual subcellular fractions were submitted to 2DGE followed by trans-blotting to a PVDF membrane. The membrane was subsequently stained to locate protein spots and phosphorimaged to locate radioactive spots. Among hundreds of protein spots seen on the blots, many (but not all) show the presence of radiolabel (Supporting Information, Figures S1–S3). Interestingly, some of the most abundant protein spots contained little or no detectable radioactivity. Such selectivity of targeting and adduction has been also observed with other hepatotoxicants,<sup>16</sup> although the reasons behind it are not well understood.

In addition to numerous discrete radioactive protein spots, the phosphorimages of the blots of the mitochondrial and microsomal fractions show a conspicuous smear of radioactivity in the low MW/low pI area that is not stained by Coomassie. A similar pattern of radioactive but apparently non-proteinaceous material was observed on blots of 2D gels of liver microsomes from TB-treated rats,<sup>7</sup> liver mitochondria from BB-treated rats,<sup>16</sup> and total protein from human hepatocytes incubated with tienilic acid.<sup>22</sup> Because this material is observed only in the membrane fractions and does not stain with Coomassie, we speculated that it might be some type of adducted lipid material. Although TASO and TB are well known to generate adducts on the amine group of PE lipids,<sup>6, 8</sup> it is not clear whether these adducts could account for the low MW/low pI material in the phosphorimage and we have not pursued this question further.

### Incubation of cells with [ $^{13}\text{C}_2\text{D}_3$ ]-TASO

To generate an isotopic signature that would facilitate detection of adducted peptides by mass spectrometry we also incubated freshly isolated hepatocytes with a mixture of TASO and [ $^{13}\text{C}_2\text{D}_3$ ]-TASO (10:6 mol ratio). The incubated cells were homogenized and centrifuged to obtain the mitochondria, microsomes and cytosol, and a portion of each

fraction was subjected to 2D gel electrophoresis as described above (6 replicate gels per fraction). Representative Coomassie-stained gels are shown in Figures S1–S3. Using the phosphorimage of the  $^{14}\text{C}$  blot as a guide, spots corresponding to radioactive target spots were excised, pooled and subjected to in-gel digestion and LC-MS/MS analysis. Because some proteins, particularly membrane proteins, do not separate well on 2DGE,<sup>23</sup> a second portion of each subcellular fraction was subjected to 1D SDS-PAGE (Figure S4), after which each lane was cut into 18 bands. Corresponding bands were pooled and subjected to in-gel digestion followed by LC-MS/MS analysis.

### Target protein identification by 2DGE and LC-MS/MS

One or more proteins were identified in each of 117 spots from the cytosol fraction, 112 spots from the mitochondrial fraction and 92 spots from the microsomal fraction (Table 2). Because some spots contained more than one identifiable protein, the total number of proteins identified in target spots (1061; Table 2 line 5) exceeded the total number of such spots (396). Approximately 25% of the spots analyzed contained only a single protein; hence that protein was taken to be a target protein even if no adducted peptides were observed. In contrast, the observation of multiple proteins in a single spot obviously raises a question about the identity of the actual target protein(s) unless adducted peptides are observed. This becomes especially important when one uses 1DGE because of its lower resolving power compared to 2DGE (see below).

To identify adducts, we first searched the mass spectra of the digests of 2DGE spots against a protein database for the presence of light/heavy pairs of acetyl- or acetimidoyl-peptides (i.e., M+42/M+47 or M+41/M+46, respectively). Examples of MS/MS spectra of peptides displaying the expected isotopic signature in both types of adducts are shown in Figure S5.

The Scaffold peptide probability scores for adducted peptides were generally at the 95% level. In a very few cases, low scores occurred when there was ambiguity in a sequence tag that would be required to correctly localize the modification to a specific amino acid (reflected in the Mascot Delta score) even though the identity scores for the reported adducted peptide was high. Thus the lowest probability scores were for adducts either involving one of a pair of two adjacent lysines, or adducts on a N-terminal residue. Independent of peptide probability scores, all the adducted peptide hits were carefully examined for sequence tags and the accuracy of their MS1 mass measurement (Table S4). The average error for adducted peptides was 2.3 ppm. An additional reliability criterion for accepting identities of adducted peptides was presence of light/heavy peptide ion pairs in the MS1 spectra, as shown by the example in Figure S6. When such pairs were found the intensities of monoisotopic peaks were taken to estimate light/heavy ratios for both acetyl- and acetimidoyl- derivatives.

The observation of both members of the isotopic pair indicates that the adduct is definitely TASO-derived, but in some cases only the light member of the light/heavy adduct pair was observed by MS/MS. Because protein acetylation is a well-known endogenous modification, the appearance of a M+42 peptide without a corresponding M+47 partner does not necessarily indicate a target protein. When we observed such occurrences the proteins were not counted as target proteins unless the modification occurred at a position neither known nor predicted to be endogenously acetylated (see proteins 12 and 65 in Table S1 for examples).

In contrast to the ambiguity of observing M+42 as the sole modification, we observed no instances of M+47 in the absence of a corresponding M+42. On the other hand, since protein acetimidoylation is not an endogenous process, the observation of either an M+41 or an M+46 acetimidoyl adduct on a lysine residue provided a clear indication that its parent protein

was a target for the reactive metabolite of TASO. Of the 88 target proteins identified, 21, 29 and 38 had zero, one or more than one observed modifications, respectively.

### Target protein identification by 1DGE and LC-MS/MS

Because of the lower resolution of 1D gels, digests of some of the bands cut from the gel contained up to 25 identifiable proteins. The total numbers of proteins identified in the three subcellular fractions after 1D vs. 2D gel electrophoresis are given in Table 2. We also observed many adduct-containing peptides in the digests of the 1D gel fractions. This is critically important for differentiating target proteins from non-target proteins in the complex digest mixtures. While many of the target proteins identified from digests of 1DGE bands are also observed in digests from 2DGE spots, several target proteins were identified only from the 1DGE data. Among these are two isoforms of cytochrome P450 (one of which, CYP2E1, is known to be involved in the bioactivation of TA and TASO),<sup>5, 24</sup> two isoforms of UGT, a mitochondrial fission protein, carboxylesterase 3 (ES-10), and several others. Although P450 and UGT enzymes have previously been identified as reactive metabolite targets, this is the first time that an adducted peptide from a P450 or UGT enzyme has been observed.

**Chemistry of adduct formation**—As shown in Scheme 1, the reactive metabolite of TASO is a S,S-dioxide that tautomerizes to form an iminosulfinic acid capable of reacting with nucleophilic amine groups on protein lysines and PE lipids to form an amidine derivative. Amidines are chemically stable and do not hydrolyze to amides under ordinary conditions. However, the iminosulfinic acid can undergo hydrolysis to form an acylsulfinic acid capable of acylating amines to form an amide derivative. An alternative hydrolysis pathway leads to acetamide as a stable metabolite. Curiously, while TB and TASO each give rise to both amide and amidine adducts on cellular proteins, their cellular PE targets show exclusively amidine modifications.<sup>5, 8</sup> In this study peptide adducts were observed and identified at 187 different positions on 67 of the 88 non-redundant TASO target proteins (Table 2, Table S1). At 36 of these positions both amide and amidine adducts were observed. As summarized in Table 2 and detailed in Table S1, a total of 173 acetylated and 51 acetimidoylated peptides was observed, thus the overall ratio of acetylation to acetimidoylation was 3.4. A similar ratio (ca. 3) was previously observed for benzoylation vs. benzimidoylation of liver proteins from TB-treated rats.<sup>7</sup> A majority of the adducts of both types were formed on the  $\epsilon$ -amino groups of lysine side chains, although both types were also observed on N-terminal amine groups, especially proline.

**Comparison of observed vs. predicted sites of acetylation**—The UniProt database predicted 38 of our 88 target proteins to have one or more (range 1–15) sites of lysine acetylation (Table S1), whereas we actually observed 54 proteins with 1 acetyl lysine (AcK) modifications (range 1–15). Out of a total of 152 observed AcK sites among these 54 proteins, only 19 individual sites were predicted by UniProt. To look more closely at the question of endogenous vs. xenobiotic acetylation we examined six representative target proteins for which the MS/MS sequence coverage was 45% and for which numerous adducted peptides were observed (Table S2). In all cases where a lysine modification was observed, peptides containing the same lysine in unmodified form were also observed. In addition, some of the predicted acetylation positions were observed in both acetylated and acetimidoylated forms. Although peak intensity ratios in mass spectrometry are not reliable indicators of molar ratios, it is worth noting that in virtually every case, the intensity of the unmodified peptide was 10–100 times as great as that of the modified peptide. On the other hand the ratio of light to heavy acetyl groups in individual AcK-containing peptides was  $2.49 \pm 1.02$  (mean  $\pm$  sd,  $n = 24$ ), and the corresponding ratio for amidine groups was  $2.27 \pm 0.44$ . These values are a little higher than the 1.67 ratio of the starting TASO. That the

light:heavy ratio in the observed AcK adducts is higher than that of the starting TASO is consistent with the occurrence of small and variable amounts of endogenous acetylation at these sites. However, this suggestion must be tempered by the observation that the light:heavy ratio is also elevated among the acetimidoyl lysine adducts, where no endogenous contribution is possible. It should be noted that among the various acetylomes that have been characterized to date,<sup>25–28</sup> none report data on the relative degree (mole fraction) of acetylation at any given site on the protein. This is largely for two reasons: one is the uncertainty about relative response factors for acetylated vs. unmodified peptide mentioned above; the other is that in most cases samples were enriched prior to analysis using an anti-AcK antibody, thereby precluding measurement of the unmodified peptide.

**Comparison of TASO-treated rat vs. normal human acetylomes—**Zhao et al. detected more than 1300 acetylated peptides representing 1047 distinct proteins, or slightly more than one acetylated peptide per protein, in normal human liver.<sup>29</sup> Of the 88 rat proteins identified as targets for TASO metabolites, 31 had human orthologs that also appeared in the list reported by Zhao et al. We selected 20 of the 31 rat proteins to analyze with respect to acetylation status as compared to predictions by UniProt and observations by Zhao et al. (Table S3). Only three of the 20 acetylated human peptides observed by Zhao et al. were predicted by UniProt to be acetylated. Of the 20 orthologous rat proteins, two did not have a lysine at the corresponding position. Among the other 18 rat peptides UniProt predicted five cases of acetylation, but none of these was observed. We observed only one case of acetylation among the 18 rat peptides (cytochrome b5, line 5). The same acetylated peptide was also observed by Zhao et al., but neither case was predicted by UniProt. However, 14 of the other 18 rat peptides were observed in unmodified form (Table S3) while in three cases no corresponding rat peptide was observed.

### Summary of TASO target protein and adduct identification

By applying the search and acceptance criteria mentioned above we identified a total of 362 adducted peptides derived from a total of 1061 target and non-target proteins (Table 2 line 5). However, there is considerable redundancy within these data resulting from the imperfect separation of the three subcellular fractions via single successive centrifugation steps, from the parallel use of both 1D and 2D electrophoresis, and because it is not uncommon for some proteins to appear in several distinct, well-separated spots on 2D gels.<sup>16, 30, 31</sup> After correcting for this redundancy a total of 187 distinct sites of adduction were observed among a total of 88 non-redundant target proteins. The latter are listed in Table 3, grouped under several subheadings according to their known cellular function; the details of the information used for their identification and the sites and nature of the adducts observed in each case are given separately in Tables S1 and S4. Of the 88 targets identified, only 21 occurred in single-protein spots on 2D gels; the others were identified by observing adducted peptides in digests of materials from 1D and/or 2D gels.

**Potential toxicological consequences of protein modification by reactive metabolites of TASO—**The largest subgroup of TASO target proteins consists of 25 enzymes of intermediary metabolism plus 13 enzymes of drug metabolism. While it is not known whether adduction by TASO actually inhibits any of these enzymes, enzyme inhibition *per se* is not likely to be a major cause of cytotoxicity in most cases, because for any given protein the average extent of adduction is very low. For example, whereas covalent binding of TASO can reach 20 nmol/mg protein, typical levels for other well known hepatotoxicants (e.g., acetaminophen or bromobenzene) are usually around 1–2 nmol/mg protein, and the levels for many other drugs are even lower.<sup>8, 32, 33</sup> Thus, for a 50 kDa protein adducted to a level of 1 nmol/mg protein, only five molecules out of 100 would actually be modified. For most pathways in most cells, 5% inhibition would not likely lead



to acute cytotoxicity, especially if that enzyme was not the rate-limiting step in the pathway. It would seem, therefore, that for covalent adduction of proteins to elicit major biological effects, some form of amplification, such as that seen in immunological responses or cell signaling cascades, would be required. Immunological reactions in patients can be triggered by metabolites in some cases (e.g. halothane or tienilic acid),<sup>34-37</sup> but for most metabolically activated pro-toxins one must look to other potential mechanisms of response amplification.

One such mechanism may arise through the effects of protein adduction on protein-protein interactions (PPIs). Proteins in cells exist in an extremely crowded environment owing to their high total concentration.<sup>38, 39</sup> Covalent adduction can alter the size, hydrophobicity and even the ionic charge of protein side chains. Such changes can alter the tertiary or even quaternary structure of proteins, leading to the inhibition of essential PPIs or the inadvertent generation of new ones (e.g. with chaperones and heat shock proteins<sup>40-43</sup> or with components of intracellular signaling pathways). Extensive evidence implicates the involvement of protein kinase-based signaling pathways such as extracellular signal-related kinase 1/2 (ERK1/2), c-Jun N-terminal kinase (JNK), and nuclear factor kappa-B (NF- $\kappa$ B) in cellular responses to toxic or reactive chemicals or metabolites.<sup>44-53</sup> Malfolded proteins disrupt ER function leading to activation of the unfolded protein response (UPR) and, in the extreme case, to apoptosis.<sup>40, 54-56</sup> Chaperones and heat shock proteins can protect cells against these deleterious effects,<sup>57-59</sup> but only up to a point, after which the cell commits to apoptosis.<sup>48, 53</sup>

The second largest group of TASSO targets consists of 18 proteins involved in protein folding and/or stress response. Within this group PDI A1 and PDI A3 stand out by becoming acylated at 10 and 15 different lysines, respectively, none of which is known to be a site of endogenous acetylation.<sup>60</sup> They are also the two most frequently reported targets for reactive metabolites in the entire TPDB, with each being attacked by 12 different chemicals.<sup>12</sup> The PDIs represent a family of multifunctional enzymes that are major components of ER protein quality control.<sup>61-63</sup> They are induced as part of stress responses and the unfolded protein response, and their induction (e.g., by heat stress) protects cells against the cytotoxic effects of agents like acetaminophen.<sup>46, 59, 64</sup> Whether their adduction by reactive metabolites generally inhibits their function is not known, but it is known that bovine PDI is adducted and inhibited by reactive electrophiles derived from lipid peroxidation.<sup>65</sup> One can speculate, therefore, that appending hydrophobic xenobiotic adducts onto these proteins may impair their ability to function normally and thereby render cells more susceptible to the harmful effects of protein adduction.

In recent years protein lysine acetylation has come to be recognized as an important mechanism for regulating the activity, stability and half-life of many cellular proteins.<sup>66, 67</sup> Large protein "acetylomes" have been described for *Salmonella*,<sup>27</sup> *Arabidopsis*,<sup>28</sup> *Drosophila*,<sup>68</sup> human liver<sup>29</sup> and several human cell lines.<sup>25, 26</sup> Histone acetylation and deacetylation regulate chromatin structure and the availability of DNA for transcription or replication.<sup>69</sup> Acetylation and de-acetylation is also a major mechanism for regulating the activity of many metabolic enzymes, especially in mitochondria.<sup>70</sup> Nearly 20% of mitochondrial proteins exhibit nutrient-dependent lysine acetylation that modulates the TCA cycle, the electron transport chain and oxidative phosphorylation, amino acid metabolism and antioxidant defenses.<sup>26, 27</sup> The sirtuin family of deacetylases depend on NAD<sup>+</sup> as a cofactor which therefore couples the energy- and redox status of the cell to the regulation of metabolic enzymes.<sup>70</sup> The X-box-binding protein 1 (XBP1), a key regulator of the unfolded protein response, is itself regulated by protein acetylation,<sup>71</sup> as are the activities of the transcription factor p53<sup>69, 72</sup> and the chaperone protein HSP90.<sup>73</sup> Given the widespread roles of protein acetylation in regulating cellular metabolism, it is not hard to imagine that

the dramatic burst of protein acetylation that accompanies the oxidation of TASO in cells (Figure 1) could lead to significant derangements of cellular homeostasis leading to cell death. Collectively, it is our opinion that xenobiotic post-translational modifications inflicted on stress response proteins, chaperones, and signaling- or regulatory proteins by chemically reactive metabolites are likely to comprise major mechanisms by which chemically reactive metabolites produce cellular injury.

## Supplementary Material

Refer to Web version on PubMed Central for supplementary material.

## Acknowledgments

### Funding Information

The work described in this manuscript was supported in part by NIH grant GM-21784.

## Abbreviations

<b>1DGE</b>	1 dimensional gel electrophoresis
<b>2DGE</b>	2 dimensional gel electrophoresis
<b>AcK</b>	acetyllysine
<b>CHAPS</b>	3-[(3-cholamidopropyl)dimethylammonio]-1-propanesulfonate
<b>DMEM</b>	Dulbecco's modified Eagle's medium
<b>DTT</b>	dithiothreitol
<b>PAGE</b>	polyacrylamide gel electrophoresis
<b>PE</b>	phosphatidylethanolamine
<b>SDS</b>	sodium dodecyl sulfate
<b>TA</b>	thioacetamide
<b>TASO</b>	thioacetamide S-oxide
<b>TB</b>	thiobenzamide
<b>UPR</b>	unfolded protein response
<b>WME</b>	Williams' Medium E

## References

1. Hunter AL, Holscher MA, Neal RA. Thioacetamide-induced hepatic necrosis. I. Involvement of the mixed-function oxidase enzyme system. *J Pharmacol Exp Therap.* 1977; 200:439–448. [PubMed: 839448]
2. Hanzlik RP, Vyas KP, Traiger GJ. Substituent effects on the hepatotoxicity of thiobenzamide derivatives in the rat. *Toxicol Appl Pharmacol.* 1978; 46:685–694. [PubMed: 746555]
3. Hanzlik RP, Cashman JR, Traiger GJ. Relative hepatotoxicity of substituted thiobenzamides and thiobenzamide-S-oxides in the rat. *Toxicol Appl Pharmacol.* 1980; 55:260–272. [PubMed: 7423516]
4. Cashman JR, Parikh KK, Traiger GJ, Hanzlik RP. Relative hepatotoxicity of ortho and meta monosubstituted thiobenzamides in the rat. *Chem-Biol Interactions.* 1983; 45:341–347.

5. Hajovsky L, Hu G, Koen Y, Sarma D, Cui W, Moore D, Staudinger J, Hanzlik RP. Metabolism and toxicity of thioacetamide and thioacetamide *S*-oxide in rat hepatocytes. *Chem Res Toxicol.* 2012; 25:1955–1963. [PubMed: 22867114]
6. Sarma D, Hajovsky H, Koen YM, Galeva NA, Williams TD, Staudinger JL, Hanzlik RP. Covalent modification of lipids and proteins in rat hepatocytes, and *in vitro*, by thioacetamide metabolites. *Chem Res Toxicol.* 2012; 25:1868–1877. [PubMed: 22667464]
7. Ikehata K, Duzhak T, Galeva NA, Ji T, Koen YM, Hanzlik RP. Protein targets of reactive metabolites of thiobenzamide in rat liver *in vivo*. *Chem Res Toxicol.* 2008; 21:1432–1442. [PubMed: 18547066]
8. Ji T, Ikehata K, Koen YM, Esch SW, Williams TD, Hanzlik RP. Covalent modification of microsomal lipids by thiobenzamide metabolites *in vivo*. *Chem Res Toxicol.* 2007; 20:701–708. [PubMed: 17381136]
9. Mangipudy RS, Chanda S, Mehendale H. Tissue repair response as a function of dose in thioacetamide hepatotoxicity. *Env Health Persp.* 1995; 103:260–267.
10. Dyroff MC, Neal RA. Identification of the major protein adduct formed in rat liver after thioacetamide administration. *Cancer Res.* 1981; 41:3430–3435. [PubMed: 6790164]
11. Dyroff MC, Neal RA. Studies on the mechanism of metabolism of thioacetamide *S*-oxide by rat liver microsomes. *Molec Pharmacol.* 1983; 23:219–227. [PubMed: 6408387]
12. ([http://tpdb.medchem.ku.edu:8080/protein\\_database/](http://tpdb.medchem.ku.edu:8080/protein_database/))
13. Sarma D, Hanzlik RP. Synthesis of carbon-14, carbon-13 and deuterium labeled forms of thioacetamide and thioacetamide *S*-oxide. *Journal of Labelled Compounds and Radiopharmaceuticals.* 2011; 54:795–798.
14. (<http://grants1.nih.gov/grants/guide/notice-files/not96-208.html>)
15. Mudra DR, Parkinson A. Preparation of hepatocytes. *Current Protocols in Toxicology.* 2001; (Supplement 8):14.12.11–14.12.13.
16. Koen YM, Gogichaeva NV, Alterman MA, Hanzlik RP. A proteomic analysis of bromobenzene reactive metabolite targets in rat liver cytosol *in vivo*. *Chem Res Toxicol.* 2007; 20:511–519. [PubMed: 17305373]
17. Koen YM, Hanzlik RP. Identification of seven proteins in the endoplasmic reticulum as targets for reactive metabolites of bromobenzene. *Chem Res Toxicol.* 2002; 15:699–706. [PubMed: 12018992]
18. Koen YM, Williams TD, Hanzlik RP. Identification of three protein targets for reactive metabolites of bromobenzene in rat liver cytosol. *Chem Res Toxicol.* 2000; 13:1326–1335. [PubMed: 11123975]
19. Olsen JV, Mann M. Improved peptide identification in proteomics by two consecutive stages of mass spectrometric fragmentation. *Proc Natl Acad Sci USA.* 2004; 101:13417–13422. [PubMed: 15347803]
20. Keller A, Nesvizhskii AI, Kolker E, Aebersold RH. Empirical statistical model to estimate the accuracy of peptide identifications made by MS/MS and database search. *Anal Chem.* 2002; 74:5383–5392. [PubMed: 12403597]
21. Nesvizhskii AI, Keller A, Kolker E, Aebersold R. A statistical model for identifying proteins by tandem mass spectrometry. *Anal Chem.* 2003; 75:4646–4658. [PubMed: 14632076]
22. Koen YM, Sarma D, Williams TD, Galeva NA, Obach RS, Hanzlik RP. Identification of protein targets of reactive metabolites of tienilic acid in human hepatocytes. *Chem Res Toxicol.* 2012; 25:1145–1154. [PubMed: 22462724]
23. Galeva NA, Alterman MA. Comparison of one-dimensional and two-dimensional gel electrophoresis as a separation tool for proteomic analysis of rat liver microsomes: Cytochromes P450 and other membrane proteins. *Proteomics.* 2002; 2:713–722. [PubMed: 12112853]
24. Chilakapati J, Korrapati MC, Shankar K, Hill RA, Warbritton A, Latendresse JR, Mehendale HM. Role of cyp2E1 and saturation kinetics in the bioactivation of thioacetamide: Effects of diet restriction and phenobarbital. *Toxicol Appl Pharmacol.* 2007; 219:72–84. [PubMed: 17234228]
25. Choudhary C, Kumar C, Gnad F, Nielsen ML, Rehman M, Walther TC, Olsen JV, Mann M. Lysine acetylation targets protein complexes and co-regulates major cellular functions. *Science.* 2009; 325:834–840. [PubMed: 19608861]

26. Kim SC, Sprung R, Chen Y, Xu Y, Ball H, Pei J, Cheng T, Kho Y, Xiao H, Xiao L, Grishin NV, White M, Yang X-J, Zhao Y. Substrate and functional diversity of lysine acetylation revealed by a proteomics survey. *Molecular Cell*. 2006; 23:607–618. [PubMed: 16916647]
27. Wang Q, Zhang Y, Yang C, Xiong H, Lin Y, Yao J, Li H, Xie L, Zhao W, Yao Y, Ning Z-B, Zeng R, Xiong Y, Guan K-L, Zhao S, Zhao G-P. Acetylation of metabolic enzymes coordinates carbon source utilization and metabolic flux. *Science*. 2010; 327:1004–1007. [PubMed: 20167787]
28. Wu X, Oh M-H, Schwarz EM, Larue CT, Sivaguru M, Imai BS, Yau PM, Ort DR, Huber SC. Lysine acetylation is a widespread protein modification for diverse proteins in arabidopsis. *Plant Physiology*. 2011; 155:1769–1778. [PubMed: 21311030]
29. Zhao S, Xu W, Jiang W, Yu W, Lin Y, Zhang T, Yao J, Zhou L, Zeng Y, Li H, Li Y, Shi J, An W, Hancock SM, He F, Qin L, Chin J, Yang P, Chen X, Lei Q, Xiong Y, Guan K-L. Regulation of cellular metabolism by protein lysine acetylation. *Science*. 2010; 327:1000–1004. [PubMed: 20167786]
30. Meier BW, Gomez JD, Zhou A, Thompson JA. Immunochemical and proteomic analysis of covalent adducts formed by quinone methide tumor promoters in mouse lung epithelial cell lines. *Chem Res Toxicol*. 2005; 18:1575–1585. [PubMed: 16533022]
31. Qiu Y, Burlingame AL, Benet LZ. Identification of the hepatic protein targets of reactive metabolites of acetaminophen *in vivo* in mice using two-dimensional gel electrophoresis and mass spectrometry. *J Biol Chem*. 1998; 273:17940–17953. [PubMed: 9651401]
32. Evans DC, Watt AP, Nicoll-Griffith DA, Baillie TA. Drug—protein covalent adducts: An industry perspective on minimizing the potential for drug bioactivation in drug discovery and development. *Chem Res Toxicol*. 2004; 17:3–16. [PubMed: 14727914]
33. Obach RS, Kalgutkar AS, Soglia JR, Zhao SX. Can *in vitro* metabolism-dependent covalent binding data in liver microsomes distinguish hepatotoxic from nonhepatotoxic drugs? An analysis of 18 drugs with consideration of intrinsic clearance and daily dose. *CRC Crit Rev Toxicol*. 2008; 21:1814–1822.
34. Zimmerman HJ, Lewis JH, Ishak KG, Maddrey WC. Ticrynafen-associated hepatic injury: Analysis of 340 cases. *Hepatology*. 1984; 4:315–323. [PubMed: 6706306]
35. You Q, Cheng L, Reilly TP, Wegmann D, Ju C. Role of neutrophils in a mouse model of halothane-induced liver injury. *Hepatology*. 2006; 44:1421–1431. [PubMed: 17133481]
36. Uetrecht J. Idiosyncratic drug reactions: Past present, and future. *Chem Res Toxicol*. 2008; 19:20–29.
37. Uetrecht J. Immune-mediated adverse drug reactions. *Chem Res Toxicol*. 2009; 22:24–34. [PubMed: 19149477]
38. Ellis RJ. Macromolecular crowding: Obvious but underappreciated. *Trends in Biochem Sci*. 2001; 26:597–604. [PubMed: 11590012]
39. Levy ED, De S, Teichmann SA. Cellular crowding imposes global constraints on the chemistry and evolution of proteomes. *Proc Natl Acad Sci USA*. 2012; 109:20461–20466. [PubMed: 23184996]
40. Balch WE, Morimoto RI, Dillin A, Kelly JW. Adapting proteostasis for disease intervention. *Science*. 2008; 319:916–919. [PubMed: 18276881]
41. Cribb AE, Peyrou M, Muruganandan S. The endoplasmic reticulum in xenobiotic toxicity. *Drug Metab Rev*. 2005; 37:405–442. [PubMed: 16257829]
42. Lewis MD, Roberts BJ. Role of cyp2E1 activity in endoplasmic reticulum ubiquitination, proteasome association, and the unfolded protein response. *Arch Biochem Biophys*. 2005; 436:237–245. [PubMed: 15797236]
43. West JD, Wang Y, Morano KA. Small molecular activators of the heat shock response: Chemical properties, molecular targets, and therapeutic promise. *Chem Res Toxicol*. 2012; 25:2035–2053.
44. Ryoo K, Huh S-H, Lee YH, Yoon KW, Cho S-G, Choi E-J. Negative regulation of mekk1-induced signaling by glutathione S-transferase mu. *J Biol Chem*. 2004; 279:43589–43594. [PubMed: 15299005]
45. Wang Y, Singh R, Kefkowitz JH, Rigoli RM, Czaja MJ. Tumor necrosis factor-induced toxic liver injury results from JNK2-dependent activation of caspase-8 and the mitochondrial death pathway. *J Biol Chem*. 2006; 281:15258–15267. [PubMed: 16571730]

46. Maniratanachote R, Minami K, Katoh M, Nakajima M, Yokoi T. Chaperone proteins involved in troglitazone-induced toxicity in human hepatoma cell lines. *Toxicol Sci.* 2005; 83:293–302. [PubMed: 15525695]
47. Hanawa N, Shinohara N, Saberi B, Gaarde WA, Han D, Kaplowitz N. Role of JNK translocation to mitochondria leading to inhibition of mitochondria bioenergetics in acetaminophen-induced liver injury. *J Biol Chem.* 2008; 283:13565–13577. [PubMed: 18337250]
48. Jones BE, Czaja MJ. Mechanisms of hepatic toxicity III. Intracellular signaling in response to toxic liver injury. *Am J Physiol.* 1998; 275:G874–G878. [PubMed: 9815013]
49. Reinehr R, Becker S, Keitel V, Eberle A, Grether-Beck S, Häussinger D. Bile salt-induced apoptosis involves NADPH oxidase isoform activation. *Gastroenterology.* 2005; 129:2009–2011. [PubMed: 16344068]
50. Niso-Santano J, Moran JM, Garcia-Rubio L, Gomez-Martin A, Gonzalez-Polo RA, Soler G, Fuentes JM. Low concentrations of paraquat induces early activation of extracellular signal-regulated kinase 1/2, protein kinase b, and c-Jun N-terminal kinase 1/2 pathways: Role of c-Jun N-terminal kinase in paraquat-induced cell death. *Toxicol Sci.* 2006; 92:507–515. [PubMed: 16687388]
51. Henderson NC, Pollock KJ, Frew J, Mackinnon AC, Flavell RA, Davis RJ, Sethi T, Simpson KJ. Critical role of c-Jun (NH2) terminal kinase in paracetamol-induced acute liver failure. *Gut.* 2007; 56:982–990. [PubMed: 17185352]
52. West JD, Marnett LJ. Endogenous reactive intermediates as modulators of cell signaling and cell death. *Chem Res Toxicol.* 2006; 19:173–194. [PubMed: 16485894]
53. Winter-Vann AM, Johnson GL. Integrated activation of map3ks balances cell fate in response to stress. *Journal of Cellular Biochemistry.* 2007; 102:848–858. [PubMed: 17786929]
54. De Camilli P, De Matteis MA. Membranes and organelles: Editorial overview. *Current Opinion in Cell Biology.* 2006; 18:349–350.
55. Horton J. Unfolding lipid metabolism. *Science.* 2008; 320:1433–1434. [PubMed: 18556540]
56. Zhao L, Ackerman SL. Endoplasmic reticulum stress in health and disease. 2006; 18:444–452.
57. Lee M-W, Park SC, Chae H-S, Bach J-H, Lee H-J, Lee SH, Kang YK, Kim KY, Lee WB, Kim SS. The protective role of hsp90 against 3-hydroxykynurenine-induced neuronal apoptosis. *Biochem Biophys Res Commun.* 2001; 284:261–267. [PubMed: 11394871]
58. Tolson JK, Dix DJ, Voellmy RW, Roberts SM. Increased hepatotoxicity of acetaminophen in hsp70i knockout mice. *Toxicol Appl Pharmacol.* 2006; 210:157–162. [PubMed: 16280147]
59. Salminen WF, Voellmy R, Roberts SM. Effect of *N*-acetylcysteine on heat shock protein induction by acetaminophen in mouse liver. *J Pharmacol Exp Therap.* 1998; 286:519–524. [PubMed: 9655897]
60. ([www.expasy.org](http://www.expasy.org))
61. Benham AM. The protein disulfide isomerase family: Key players in health and disease. *Antioxid Redox Signal.* 2012; 16:781–789. [PubMed: 22142258]
62. Imaoka S. Chemical stress on protein disulfide isomerases and inhibition of their functions. *Int Rev Cell Mol Biol.* 2011; 290:121–166. [PubMed: 21875564]
63. Smathers RL, Galligan JJ, Stewart BJ, Petersen DR. Overview of lipid peroxidation products and hepatic protein modification in alcoholic liver disease. *Chem-Biol Interactions.* 2011; 192:107–112.
64. Salminen WF, Voellmy R, Roberts SM. Protection against hepatotoxicity by a single dose of amphetamine: The potential role of heat shock protein induction. *Toxicol Appl Pharmacol.* 1997; 147:247–258. [PubMed: 9439720]
65. Carbone DL, Doorn JA, Kiebler Z, Petersen DR. Cysteine modification by lipid peroxidation products inhibits protein disulfide isomerase. *Chem Res Toxicol.* 2005; 18:1324–1331. [PubMed: 16097806]
66. Close P, Creppe C, Gillard M, Ladang A, Chapelle J-P, Nguyen L, Chariot A. The emerging role of lysine acetylation of non-nuclear proteins. *Cellular and Molecular Life Sciences.* 2010; 67:1255–1264. [PubMed: 20082207]
67. Norvell A, McMahon SB. Rise of the rival. *Science.* 2010; 327:964–965. [PubMed: 20167774]

68. Weinert BT, Wanger SA, Horn H, Henriksen P, Liu WR, Olsen JV, Jensen LJ, Choudhary C. Proteome-wide mapping of the drosophila acetylome demonstrates a high degree of conservation of lysine acetylation. *Science Signaling*. 2011; 4:ra48. [PubMed: 21791702]
69. Yang X-J, Seto E. Lysine acetylation: Codified crosstalk with other posttranslational modifications. *Molecular Cell*. 2008; 31:449–461. [PubMed: 18722172]
70. Bao J, Sack MN. Protein deacetylation by sirtuins: Delineating a post-translational regulatory program responsive to nutrient and redox stressors. *Cellular and Molecular Life Sciences*. 2010; 67:3073–3087. [PubMed: 20680393]
71. Wang F-M, Chen Y-J, Ouyang H-J. Regulation of unfolded protein response modulator XBP1s by acetylation and deacetylation. *Biochem J*. 2011; 433:245–252. [PubMed: 20955178]
72. Tang Y, Zhao W, Chen Y, Zhao Y, Gu W. Acetylation is indispensable for p53 activation. *Cell*. 2008; 133:612–626. [PubMed: 18485870]
73. Scroggins BT, Robzyk K, Wang D, Marcu MG, Tsutsumi S, Beebe K, Cotter RJ, Felts S, Toft D, Karnitz L, Rosen N, Neckers L. An acetylation site in the middle domain of hsp90 regulates chaperone function. *Molecular Cell*. 2007; 25:151–159. [PubMed: 17218278]

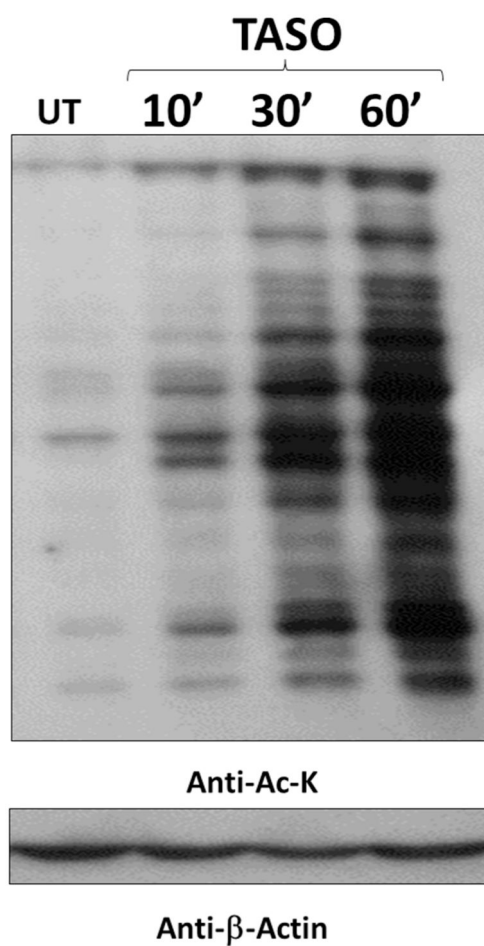
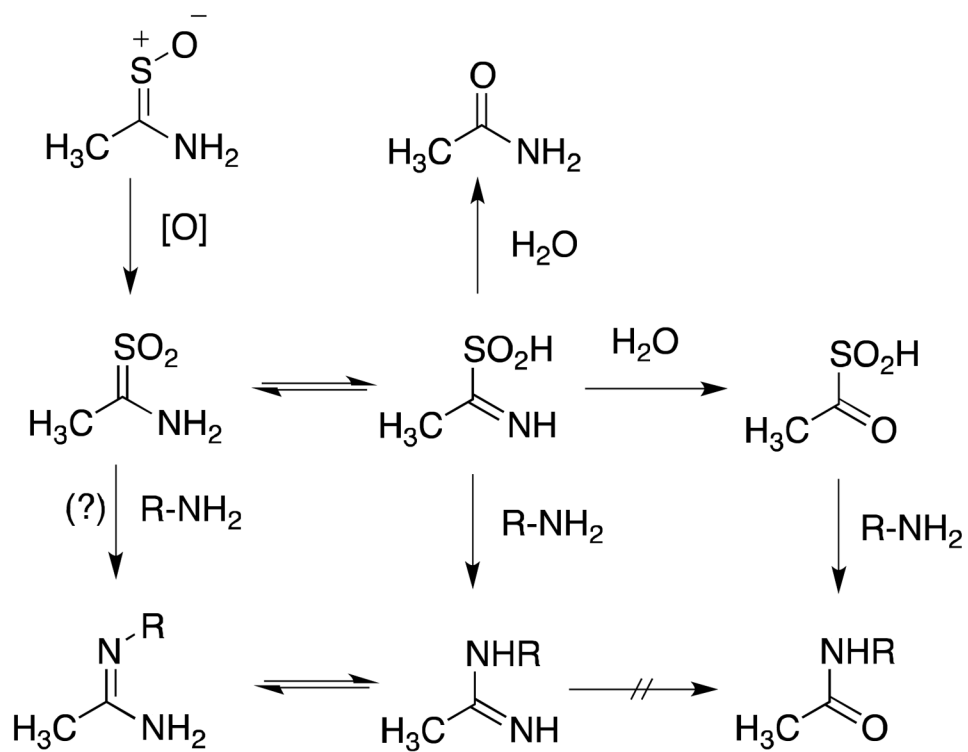


**Figure 1. Western blot showing the time-dependent increase in acetylated protein lysine side chains in rat hepatocytes treated with TASO**

Rat hepatocytes ( $1.5 \times 10^6$  cells/well) in 6-well collagen-coated plates were treated with TASO (3 mM) for the indicated times. The untreated (UT) control group was harvested at the 60 min endpoint. Whole cell lysates and western blots to detect acetylated lysine and  $\beta$ -actin were produced as described in Materials and Methods.



**Scheme 1.**  
Routes of formation and decomposition of TASO<sub>2</sub>.



Table 1

Fractionation of hepatocytes after incubation with [ $^{14}\text{C}$ ]-TASO.

Fraction	volume, mL	protein, mg/mL	total protein, mg	yield, mg protein/ $10^6$ cells	nmol-equiv. $^{14}\text{C}$ /mg protein <sup>a</sup>
mitochondria	0.41	22.2	9.0	0.09	79.8 <sup>a</sup>
microsomes	0.09	29.7	2.7	0.03	86.0 <sup>a</sup>
unfiltered cytosol	2.05	7.0	14.3	0.14	125 <sup>a,b</sup>
filtered cytosol	0.41	26.1	10.7	0.11	3.2 <sup>b</sup>

<sup>a</sup> Radioactivity was measured directly in whole samples without precipitating and washing protein.

<sup>b</sup> To remove unbound radioactivity (small molecules), 1.53 ml of unfiltered cytosol was submitted to repetitive ultrafiltration/concentration to give a final volume of 0.41 ml of filtered cytosol.

Table 2

Summary of TASO target proteins identified in rat hepatocytes.

	Cytosol	Mitochondria	Microsomes
<b>Analysis by 2DGE</b>			
protein spots observed on 2D gel	>1000	>500	>500
radioactive spots	131	137	128
spots collected for analysis	122	114	99
spots with proteins identified	117	112	92
total proteins identified <sup>a</sup>	305	534	222
target proteins identified <sup>b</sup>	77	85	71
adducted peptides identified	74	92	61
acetylated peptides	43	76	56
acetimidoylated peptides	31	16	5
<b>Analysis by 1DGE</b>			
total proteins identified	418	608	494
target proteins identified	38	39	13
adducted peptides identified	48	49	28
acetylated peptides	39	36	26
acetimidoylated peptides	9	13	2
<b>Target Proteins Observed<sup>c</sup></b>			
observed from 2DGE	33	34	34
observed from 1DGE	27	34	15
observed by both 2DGE and 1DGE	12	16	7
total number of proteins observed <sup>c</sup>	48	52	42

Total Non-Redundant Target Proteins and Peptide Adducts			
proteins	acetyl-adducts	amidine-adducts	both, acetyl and amidine
88	174	50	37
			added positions
			187
			Ratio acetyl/amidine
			3.5

<sup>a</sup>Some radioactive spots contained only a single protein but others contained from 2–5 proteins.

<sup>b</sup> Target proteins were identified either as the only protein in a radioactive spot or by observing and sequencing an adducted peptide.

<sup>c</sup> Some proteins were identified multiple times because of a) their natural distribution among subcellular fractions, b) carryover during separation of subcellular fractions, c) the distribution of some proteins into multiple spots on 2DGE, and d) the analysis of each subcellular fraction by two methods (i.e., IDGE and 2DGE).

**Table 3**

Proteins identified as targets of TASO metabolites in rat hepatocytes.

Protein name	Acc # <sup>a</sup>	Source/method <sup>b</sup>	Also target for <sup>c</sup>
<b>Intermediary metabolism (25 proteins)</b>			
3-ketoacyl-CoA thiolase A, peroxisomal	P21775	Ct9, Mt8 (1D); Ct36, Mt47, 53-57; Ms56 (2D)	
3-ketoacyl-CoA thiolase B, peroxisomal	P07871	Ct9 (1D), Ct56 (2D)	
Adenosylhomocysteinase	P10760	Ct10 (1D)	
Alcohol dehydrogenase 1	P06757	Ct9 (1D)	MDAB, <b>TB</b> , TEU
Aldehyde dehydrogenase family 8 member A1	Q9H2A2	Ct11 (1D)	
Alpha-enolase	P04764	Ct28-30; Mt44, Ms35,37 (2D)	BB, MYCO, <b>TB</b> , DACT, BHT
Arginase-1	P07824	Ct35, 36, 41; Ms53, 54 (2D)	BB, TB, TIE
Betaine--homocysteine S-methyltransferase 1	O09171	Ct10, Mt9 (1D); Mt114 (2D)	TEU
Carbamoyl-phosphate synthase	P07756	Mt12-14, Ms14 (1D)	TEU
Carbonic anhydrase 3	P14141	Ct7, Mt7 (1D); Ct21-23, 74-77; Mt33, 34, 36, 96, 97, 99; Ms86 (2D)	APAP, BB, <b>TB</b> , VCN
Carboxylesterase 3 (ES-10)	P16303	Mt10, Ms10 (1D)	MOL, BB
Cytosol aminopeptidase	Q68FS4	Ms34 (2D)	
D-dopachrome decarboxylase	P80254	Ct1-3, Mt2, 3, Ms3 (1D); Ct109, 112, 114, 116; Mt113-116; Ms112, 114, 117 (2D)	BB, <b>TB</b> , TIE
Fructose-bisphosphate aldolase B	P00884	Ct9 (1D); Ct56, Mt44, 54 (2D)	MYCO, <b>TB</b> , TEU
Fumarylacetoacetase	P25093	Ms47, 48	BB, 4BP, <b>TB</b> , TIE
Glyceraldehyde-3-phosphate dehydrogenase	P04797	Ct9 (1D); Ct43, 44, 53; Mt58, 59; Ms61, 63 (2D)	APAP, ACRM, MYCO, <b>TB</b> , TEU
Glycine N-methyltransferase	P13255	Ct8 (1D), Ct53, 54 (2D)	
Hexose-6-phosphate dehydrogenase	D4A7D7	Mt12 (1D)	
L-Lactate dehydrogenase A-chain	P04642	Ct8 (1D)	
Long-chain-fatty-acid--CoA ligase 1	P18163	Mt11 (1D)	TEU
Malate dehydrogenase, cytoplasmic	O88989	Ct47, 49 (2D)	4BP, <b>TB</b> , TIE
Methylmalonate-semialdehyde dehydrogenase	Q02253	Mt37 (2D)	MYCO, TEU
Phosphoglycerate kinase 1	P16617	Mt50, Ms51 (2D)	BB, <b>TB</b> , DACT
Triosephosphate isomerase	P48500	Ct75 (2D)	BB, 4BP, DACT, MYCO, TIE
UMP-CMP kinase	Q4KM73	Ct63, 66 (2D)	
<b>Protein synthesis (6 proteins)</b>			
40S ribosomal protein S13	P62278	Ms5 (1D)	
40S ribosomal protein S2	P27952	Ct128 (2D)	
DNA-directed RNA-polymerase III subunit RPC2	P59470	Ct82 (2D)	
Elongation factor 1-alpha 1	P62630	Ct11, Mt12 (1D)	BENZ, BHT, MYCO
Elongation factor 1-beta	O70251	Mt68 (2D)	

Protein name	Acc # <sup>a</sup>	Source/method <sup>b</sup>	Also target for <sup>c</sup>
Ribonuclease UK114	P52759	Ct1-3, Mt2, 3 (1D); Ct109, 110; Mt113, 115, 134; Ms112, 119 (2D)	BB, <b>TB</b> , MYCO
<b>Protein folding/stress response (18)</b>			
10 kDa heat shock protein, mitochondrial	P26772	Ct130 (2D)	BENZ
60 kDa heat shock protein, mitochondrial	P63039	Ct13 (2D)	NAPH, TFEC, TEU, DACT, 4BP, COC, BQ, 1,4-NQ
78 kDa glucose-regulated protein	P06761	Mt66,104; Ms9,10 (2D); Ms11 (1D)	HAL, BB, NAPH, <b>TB</b> , TEU, 4BP
Endoplasmic reticulum resident protein 29 (ERp29)	P52555	Mt76, 81, 92; Ms73, 74, 79 (2D)	BB, <b>TB</b>
Hypoxia up-regulated protein 1	Q63617	Ms13 (1D)	<b>TB</b>
Heat shock cognate 71 kDa protein	P63018	Ct13, Mt11 (1D)	BB, MYCO, <b>TB</b> , BHT, NAPH
Mesencephalic astrocyte-derived neurotrophic factor	P0C5H9	Mt118, 120, 121; Ms92 (2D)	
Peptidyl-prolyl cis-trans isomerase A	P10111	Mt5 (1D); Ct98-102; Mt122, 125-128; Ms98-101 (2D)	<b>TB</b>
Peptidyl-prolyl cis-trans isomerase B	P24368	Mt5, 6; Ms5 (1D); Mt118, 124; Ms92, 94 (2D)	<b>TB</b>
Peptidyl-prolyl cis-trans isomerase FKBP1A	Q62658	Mt3, Ms3 (1D); Mt130 (2D)	
Peptidyl-prolyl cis-trans isomerase FKBP2	D3ZZR9	Mt2, Ms3 (1D); Mt135, Ms127 (2D)	<b>TB</b>
Protein disulfide-isomerase (PDIA1)	P04785	Mt10 (1D), Mt3, 5; Ms22 (2D)	APAP, AMAP, BENZ, NAPH, HAL, MCTP, BQ, 1,4-NQ, BB, 4BP, <b>TB</b>
Protein disulfide-isomerase A3 (ER-60)	P11598	Mt10, Ms10 (1D); Mt23-29, 70, 71; Ms11-15, 17, 18 (2D)	APAP, ATRZ, DACT, NAPH, MCTP, BQ, 1,4-NQ, BB, 4BP, MYCO, <b>TB</b>
Protein disulfide-isomerase A6 (CaBP1)	Q63081	Mt47, Ms26 (2D)	BB, <b>TB</b> , TEU
Stress-70 protein, mitochondrial (75 kDa GRP, mortalin)	P48721	Mt8 (2D)	4BP, NAPH, DACT, TFEC, BQ, 1,4-NQ
Stress-induced-phosphoprotein 1	O35814	Ct8-10 (2D)	<b>TB</b>
T-complex protein 1 subunit beta	Q5XIM9	Ms32 (2D)	
UDP-glucose:glycoprotein glucosyltransferase 1	Q9JLA3	Mt14 (1D)	HAL
<b>Binding/carrier proteins (15)</b>			
Acyl-CoA-binding protein	P11030	Ct126, 127, 129; Mt136; Ms121, 128 (2D)	<b>TB</b>
Alpha-1-antiproteinase	P17475	Ms30, 31 (2D)	NAPH, AMAP, <b>TB</b>
Alpha-tocopherol transfer protein	P41034	Ct7 (1D)	
Annexin A6 (Ca-BP 65/67)	P48037	Ct13 (1D)	
Apolipoprotein A-I	P04639	Mt73, 75 (2D)	BHT, <b>TB</b>
Calnexin	P35565	Ms11 (1D)	
Calreticulin	P18418	Ms21, 23 (2D)	APAP, HAL, <b>TB</b>
Destrin (Actin-depolymerizing factor)	Q7M0E3	Ct86 (2D)	
Fatty acid-binding protein, liver	P02692	Ct1-3, Mt2,3, Ms3 (1D); Ct114, 115, 117, 118, 131; Mt113, 115, 117, 130, 131; Ms118, 122 (2D)	BB, <b>TB</b> , TIE
Histidine triad nucleotide-binding protein 1	P62959	Ct95 (2D)	

Protein name	Acc # <sup>a</sup>	Source/method <sup>b</sup>	Also target for <sup>c</sup>
Regucalcin	Q03336	Ct8 (1D), Ct61 (2D)	BB, TIE
Retinol-binding protein 4	P04916	Ms82 (2D)	
Serotransferrin	P12346	Mt19, Ms40 (2D)	COC, <b>TB</b>
Serum albumin	P02770	Ct1, 3-5, 7, 25-27; Mt11-17; Ms1-6, 8 (2D)	ATRZ, BB, 4BP, DCE, TIE, <b>TB</b> , NAPH, BFP, FCXC
Transthyretin	P02767	Mt110, 111; Ms113 (2D)	BB, <b>TB</b>
<b>Redox regulation (7 proteins)</b>			
Catalase	P04762	Ct12, Mt11 (1D); Ct20; Mt30, 32, 34; Ms42-44 (2D)	4BP, TEU, <b>TB</b>
Glutathione peroxidase 1	P04041	Ms84 (2D)	APAP
Peroxiredoxin-1	Q63716	Ct82, 84; Mt118, Ms90 (2D)	<b>TB</b> , APAP
Peroxiredoxin-4	Q9Z0V5	Ms72, 75, 78 (2D)	<b>TB</b>
Peroxiredoxin-6	O35244	Ct64, 67 (2D)	<b>TB</b> , BHT, NAPH, MYCO, ATRZ
Superoxide dismutase [Cu-Zn]	P07632	Ct91, 94; Mt107, 109 (2D)	BHT, <b>TB</b> , TIE
Thioredoxin	P11232	Ct103, 104, 108 (2D)	BB, <b>TB</b> , MCTP
<b>Xenobiotic metabolism (13 proteins)</b>			
Cytochrome b5	P00173	Mt4 (1D), Ms104 (2D)	
Cytochrome P450 2D26	P10634	Mt9 (1D)	
Cytochrome P450 2E1	P05182	Mt9,10; Ms9 (1D)	HAL
Glutathione S-transferase alpha-1 (ligandin)	P00502	Ct6, Mt3, 5, 6 (1D)	BB, MYCO
Glutathione S-transferase alpha-2 (ligandin)	P04903	Ct1, 3-6 (1D)	BB
Glutathione S-transferase alpha-3	P04904	Ct6, Mt6 (1D); Mt102 (2D)	BB
Glutathione S-transferase Mu 1	P04905	Ct6, Mt6, Ms6 (1D); Ct76, Mt96, Ms85 (2D)	BB, VCN, <b>TB</b> , TEU
Glutathione S-transferase Mu 2	P08010	Ct6, Mt6 (1D), Ct76, Mt102, Ms85 (2D)	BB, 4BP, <b>TB</b>
Glutathione S-transferase theta-2	P30713	Ct6, Mt6 (1D)	
Glutathione S-transferase Yb-3 (GST mu-3)	P08009	Ct6, Mt6 (1D)	
Liver carboxylesterase 4	Q64573	Mt10 (1D)	BB, HAL
UDP-glucuronosyltransferase 2B15	P36511	Mt9, Ms9 (1D)	
UDP-glucuronosyltransferase 2B2	P08541	Mt10 (1D)	
<b>Apoptosis related proteins</b>			
Cytochrome c, somatic	P62898	Mt135 (2D)	
Mitochondrial fission 1 protein	P84817	Mt4 (1D)	
<b>Miscellaneous proteins</b>			
Macrophage migration inhibitory factor	P30904	Mt2 (1D)	BB
Membrane-associated progesterone receptor component 1	P70580	Ms70 (2D)	

<sup>a</sup>UniProt protein databank accession number ([www.uniprot.org](http://www.uniprot.org)).

<sup>b</sup>Subcellular fraction where the protein was observed: Ct, cytosol; Mt, mitochondria; Ms, microsomes. Method used for protein separation: 1D, SDS-PAGE (i.e. 1DGE); 2D, 2-dimensional electrophoresis (2DGE).

<sup>c</sup>Other chemicals whose reactive metabolites are also known to form adducts to proteins reported here to be targeted by TASO ([http://tpdb.medchem.ku.edu:8080/protein\\_database](http://tpdb.medchem.ku.edu:8080/protein_database)). Abbreviations used: ACRM, acrylamide; AMAP, 3-hydroxyacetanilide; APAP, acetaminophen; ATRZ, atrazine; 4BP, bromophenol; BB, bromobenzene; BENZ, benzene; BFP, sarin analog; BHT, 2,5-di-*tert*-butyl-4-hydroxytoluene; BQ, 1,4-benzoquinone; CAM, chloramphenicol; COC, cocaine; DACT, diaminochlorotriazine; DCE, 1,1-dichloroethylene; FCXC, flucloxacillin; HAL, halothane; MCTP, monocrotaline pyrrole; MDAB, 3'-methyl-N,N-dimethyl-4-aminoazobenzene; MOL, molinate; MYCO, mycophenolic acid; 1,4-NQ, 1,4-naphthoquinone; NAPH, naphthalene; TB, thiobenzamide; TEU, teucrine A; TFEC, S-(1,1,2,2-tetrafluoroethyl)-L-cysteine; TIE, tienilic acid; VCN, acrylonitrile.